Supporting Information

Ortho-B-π-B-Regulated Multiple-Resonance Emitter Enables High Efficiency Narrowband Yellow OLEDs

Tao Hua,[†a] Yongxu Hu,[†a] Ting Jiang,[†a] Xiaoyu Guo,[a] Chi Zhang,[a] Zhanxiang Chen,[a] Jingsheng Miao,[a] Chuluo Yang,[a] and Zhongyan Huang*[a]

[1] *Shenzhen Key Laboratory of New Information Display and Storage Materials, College of Materials Science and Engineering, Shenzhen University, Shenzhen 518060, People's Republic of China.*

Email: zyhuang@szu.edu.cn

[†] *These authors contribution equally*

General Information

Unless otherwise stated, all chemicals and reagents were purchased from commercial suppliers without further purification. Air-sensitive reactions were conducted under a nitrogen atmosphere, and no special precautions were taken to prevent exposure to air or moisture during workups. ^{1}H NMR and ^{13}C spectra were conducted on a Bruker 400 MHZ spectrometer. The high-resolution mass spectrometry (HR-MS) of the compounds was conducted on a Thermo Scientific LTQ Orbitrap XL with an ESI ion source.

Quantum Chemical Calculations

All of the simulation calculations were carried out with Gaussian 16 program package[1]. The ground-state geometries were optimized using DFT at the B3LYP/6-31G(d,p) level. The HOMO and LUMO distributions were obtained based on the optimized geometries, and excited-state properties were evaluated by TD-DFT calculations at the same level. The ΔE_{ST} values of three MR-TADF emitters were estimated through high-level Spin-Component Scaling second-order approximate Coupled-Cluster (SCS-CC2) calculations, which was performed using the MRCC Program with cc-PVDZ method. The SOC constants were calculated using the PBE0 functional and def2-SVP basis set with the PySOC package.

Thermal and Electrochemical Characterization

Thermogravimetric analysis (TGA) was conducted using TGA-Q50 Instrument (TA Instruments, America) at a heating rate of 10 °C/min from 50 to 800 °C under a nitrogen flow environment. The thermal decomposition temperatures (T_d) were determined by the recorded temperature at 5% weight loss.

Cyclic voltammetry (CV) measurements were carried out on a CHI600 electrochemical analyzer (Chenhua, China) at room temperature, with a conventional three-electrode system, which consists of a glassy carbon as working electrode, a platinum wire as auxiliary electrode, and an Ag/AgCl standard electrode using as the reference electrode. 0.1 M tetrabutylammonium hexafluorophosphate (Bu_4NPF_6) was used as the supporting electrolyte, and ferrocene was

added as a calibrant. HOMO energy was calculated from the oxidation potential with the formula of E_{HOMO} = -[E_{ox} - E_{Fc/Fc^+} + 4.8] eV. The LUMO energy levels of three compounds were then deduced from the HOMO levels and the energy gap between HOMO and LUMO level (E_{LUMO} = E_{HOMO} - E_g). The energy gap (E_g) of HOMO and LUMO was calculated from the onset of the absorption spectrum with the formula of E_g = 1240/λ onset and LUMO energy was calculated from E_{HOMO} - E_g.

Photophysical Characterization

The UV-vis absorptionwere measured in toluene by Shimadzu UV-2600 spectrophotometer (Shimadzu, Japan) at 300 K with a concentration of 1 × 10^{-5} M. The PL spectra were recorded on a Hitachi F-7100 fluorescence spectrophotometer using an excitation wavelength of 300 nm. The room-temperature fluorescence spectra were collected at 300 K, while the low-temperature fluorescence and phosphorescence spectra were recorded at 77 K. The PL quantum efficiencies (PLQY, Φ_{PL}s) were achieved on a Hamamatsu UV-NIR absolute PL quantum yield spectrometer (C13534, Hamamatsu Photonics) equipped with an integrating sphere purged with dry argon to maintain an inert atmosphere. The transient PL decay measurements of doped films were completed by FluoTime 300 (PicoQuant GmbH) with a Picosecond Pulsed UV-LASTER (LASTER375) as the excitation source and conducted under an inert atmosphere.

Single Crystal X-ray Crystallographic Data

X-ray single crystal data of **QuBN** was identified on a Bruker D8 Venture diffractometer using MoK radiation (λ = 0.71073) source. The selected crystal was kept at 150.0 K during data collection. Using Olex2 the structure was solved with the ShelXT structure solution program using Intrinsic Phasing and refined with the ShelXL refinement package using Least Squares minimization. Selected crystal data and experimental details are listed below. All crystallographic information in CIF format have been deposited at the Cambridge Crystallographic Data Center (CCDC) under deposition number 2545133 for **QuBN**, via www.ccdc.cam.ac.uk/data_request/cif.

Analysis of Rate Constants

The rate constants of intersystem crossing (k_{ISC}) and reverse intersystem crossing (k_{RISC}) were calculated from the following six equations:

$k_p = 1/\tau_p$ .....Eq.(1)

$k_d = 1/\tau_d$ .....Eq.(2)

$k_{r,s} = \Phi_p k_p + \Phi_d k_d \approx \Phi_p k_p$ .....Eq.(3)

$$k_{nr,s} = \frac{1 - \Phi_{PL}}{\Phi_{PL}} k_{r,s}$$ .....Eq.(4)

$k_{ISC} = k_p - k_{r,s} - k_{nr}$ .....Eq.(5)

$k_{RISC} = (k_p k_d \Phi_d) / (k_{ISC} \Phi_p)$ .....Eq.(6)

where the τ_p and τ_d represent the prompt and decay fluorescence lifetimes, respectively, which were determined from transient PL spectra. The k_p and k_d represent the decay rate constants for prompt and delayed fluorescence, respectively. Φ_p and Φ_d indicate prompt and delayed fluorescence components and can be distinguished from the total Φ_{PL} by comparing the integrated intensities of prompt and delayed components in the transient PL spectra.

Device Fabrication and Measurement

The device fabrication was adopted the Proven Process in our previous work. ITO coated glass substrates with a sheet resistance of 15 Ω square^{-1} were consecutively ultrasonicated with acetone/ethanol and dried with nitrogen gas flow, followed by 20 min ultraviolet light-ozone (UVO) treatment in a UV-ozone surface processor (PL16 series, Sen Lights Corporation). Then the sample was transferred to the deposition system. Both 8-hydroxyquinolinolato-lithium (Liq) as electron injection layer and aluminum (Al) as cathode layer were deposited by thermal evaporation at 5×10^{-5} Pa. The organic layers were deposited at the rates of 0.2-3 Å/s. After the organic film deposition, Liq and Al layer were deposited with rates of 0.1 and 3 Å/s, respectively. For all the OLEDs, the emitting areas were determined by the overlap of two electrodes as 0.09 cm^2. The as-fabricated devices were measured in ambient environment without any encapsulation. The current density-voltage-luminance (*J-V-L*), *L-EQE* curves and electroluminescence spectra were measured using a Keithley 2400 source meter and an absolute

EQE measurement system (C9920-12, Hamamatsu Photonics, Japan).

Synthesis routes and procedures

The detailed procedures for the synthesis of **QuBN and DoBN** are depicted in Scheme S1-S2. The borylated precursors were synthesized from commercially available starting materials using nucleophilic substitution reactions and Buchwald-Hartwig C-N coupling reactions. The compared compound **DoBN** were synthesized according to the previously reported methods[3].

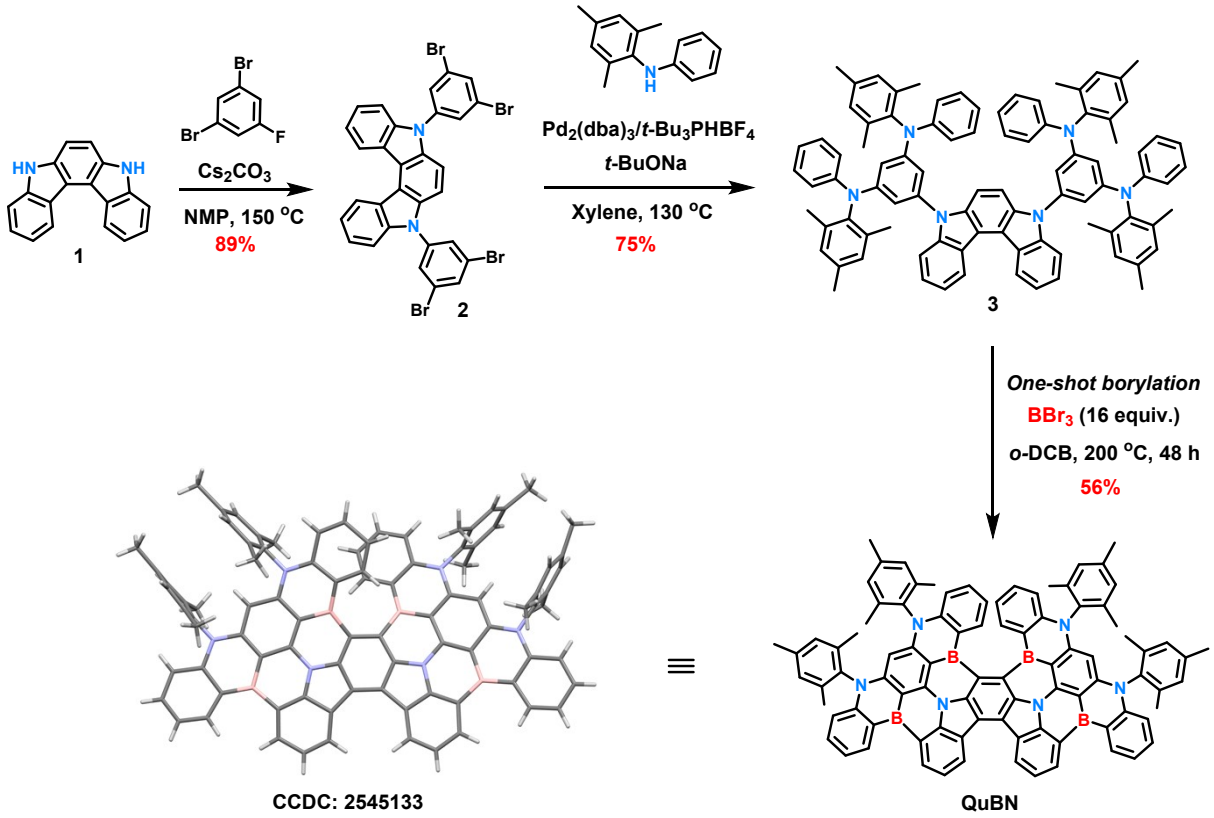

Scheme S1. The synthetic route and single crystal structure of **QuBN**.

Synthesis of 5,8-bis(3,5-dibromophenyl)-4a,5,8,12d-tetrahydroindolo[2,3-c]carbazole (**2**)

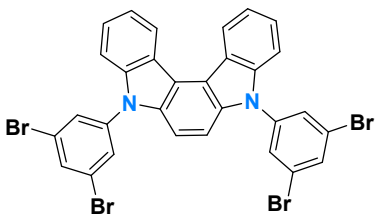

Under argon atmosphere, 4a,5,8,12d-tetrahydroindolo[2,3-*c*]carbazole (**1)** (513 mg, 2 mmol), 1,3-dibromo-5-fluorobenzene (1.0 g, 4.1 mmol) and Cs_2CO_3 (2.6 g, 8 mmol) were added into a two necked round bottom flask. Addition of NMP (30 mL) was added into the flask and the mixture was stirred for 48 hours at 150 °C. After cooling to room temperature, the mixture was poured into water and the crude product was obtained by filtration followed by washing with ethanol for three time. Intermediate **2** (1.3 g, 89%) was acquired as pale grey solid, and the product was subjected to the next step without further purification.

Synthesis of 5,5'-(indolo[2,3-c]carbazole-5,8-diyl)bis(N1,N3-dimesityl-N1,N3-diphenyl benzene-1,3-diamine) (**3**)

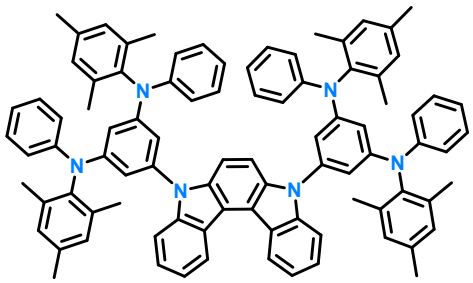

Under argon atmosphere, 2,4,6-trimethyl-N-phenylaniline (887 mg, 4.2 mmol), compound **1** (724 mg, 1 mmol), tris(dibenzylideneacetone)dipalladium (100 mg), sodium *tert*-butylate (768 mg, 8 mmol) and *tri-tert*-butylphosphine tetrafluoroborate (1.99 g, 3.70 mmol) were added into a dried 100 mL two-necked round bottom flask. After being evacuated and backfilled with nitrogen (3 times), deoxygenated xylene (30 mL) were added. The reaction mixture was stirred at 130 °C for 4 h. After being cooled down to room temperature, the xylene was removed under reduced pressure and the reaction mixture was extracted with dichloromethane for three times. The residue was purified by flash column chromatography on silica gel, compound **2** was obtained as a gray solid (635 mg, 56%). ^{1}H NMR (500 MHz, $CDCl_3$) δ 8.79 (d, J = 7.5 Hz, 2H), 7.42–7.31 (m, 8H), 7.17 (d, J = 6.8 Hz, 2H), 7.03 (d, J = 4.3 Hz, 8H), 6.97 (d, J = 2.0 Hz, 1H), 6.87–6.81 (m, 12H), 6.50 (d, J = 1.0 Hz, 4H), 2.24 (s, 12H), 2.05 (s, 24H).

Synthesis of 8,10,19,21-tetramesityl-8,10,19,21-tetrahydro-3a2,8,10,14d2,19,21-hexaaza-3b,14b,14e,25b-tetraboradiindeno[4',3',2',1':11,12,13;1'',2'',3'',4'':14,1,2]piceno[3,4,5,6-fghi:7,8,9,10-f'g'h'i']dipentacene (**QuBN**)

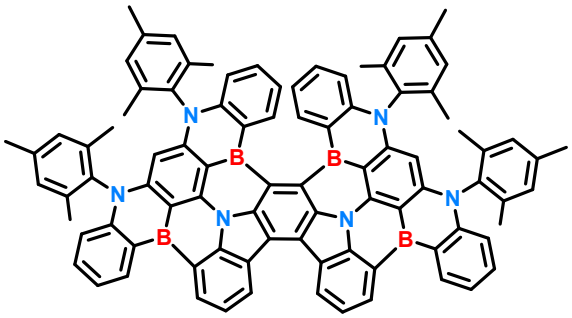

Under N_2 atmosphere, a dried 50 mL sealed tube was charged with compound **3** (622 mg, 0.5 mmol), after being evacuated and backfilled with N_2 for 3 times, ultradry *o*-dichlorobenzene (10 mL) and 0.76 mL boron tribromide (BBr_3) were added subsequently. The reaction mixture was stirred at 200 °C for 48 h. After being cooled down to room temperature, excessive BBr_3 was slowly quenched by methanol in ice water bath. The reaction mixture was concentrated under reduced pressure. The residue was purified by flash column chromatography on silica gel and recrystallized from a solution of dichloromethane and methanol to provide **QuBN** as orange-yellow solid (357 mg, 56%). ^{1}H NMR (400 MHz, $CDCl_3$) δ 8.36 (dd, J = 7.6, 1.6 Hz, 2H), 8.04 (d, J = 7.2 Hz, 2H), 7.57–7.49 (m, 2H), 7.40 (d, J = 7.6 Hz, 2H), 7.12–6.86 (m, 12H), 6.63 (d, J = 8.4 Hz, 2H), 6.35 (d, J = 7.2 Hz, 2H), 5.49 (s, 2H), 2.46 (d, J = 3.6 Hz, 12H), 2.13 (s, 6H), 1.86 (s, 6H), 1.79 (s, 6H), 1.70 (s, 6H). ^{13}C NMR (125 MHz, $CDCl_3$) δ 149.95, 149.81, 146.01, 144.75, 142.73, 142.54, 140.75, 139.75, 138.05, 137.91, 137.29, 136.88, 136.66, 136.48, 136.44, 136.24, 135.46, 134.16, 131.55, 130.36, 129.89, 129.81, 129.66, 129.33, 126.87, 124.71, 123.12, 122.90, 120.41, 118.78, 115.79, 114.18, 90.24, 21.30, 17.43, 17.33, 17.16.

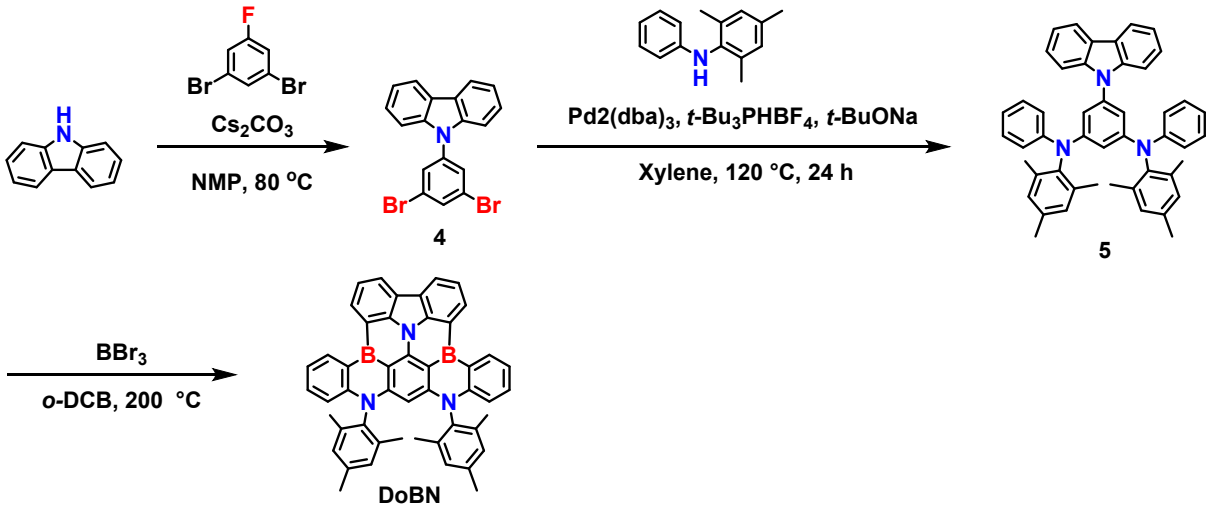

Scheme S2. The synthetic route of **DoBN**.

Synthesis of 9-(3,5-dibromophenyl)-9H-carbazole **(4)**

Intermediate **4** was synthesized according to the similar procedure of compound **2** by using carbazole (401 mg, 1 mmol) instead of 4a,5,8,12d-tetrahydroindolo[2,3-*c*]carbazole.

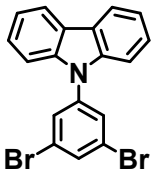

Compound **4** was obtained as a white solid in 89% yield. ^{1}H NMR (500 MHz, $CDCl_3$) δ 8.13 (d, J = 8.0 Hz, 2H), 7.77 (d, J = 1.8 Hz, 1H), 7.70 (d, J = 2.0 Hz, 2H), 7.48–7.39 (m, 4H), 7.35–7.29 (m, 2H).

Synthesis of 5-(9H-carbazol-9-yl)-N1,N3-dimesityl-N1,N3-diphenylbenzene-1,3-diamine **(5)**

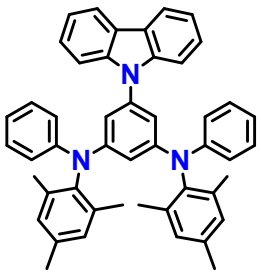

Compound **5** was synthesized according to the similar procedure of compound **3** by using compound **2** (401 mg, 1 mmol) instead of compound **1**. Precursor **4** was obtained as a white solid in 61% yield. ^{1}H NMR (500 MHz, $CDCl_3$) δ 8.04 (d, J = 7.0 Hz, 2H), 7.35–7.25 (m, 4H),

7.25–7.13 (m, 6H), 7.02 (d, *J* = 9.0 Hz, 4H), 6.94 (d, *J* = 2.3 Hz, 1H), 6.46 (d, *J* = 2.0 Hz, 2H), 2.26 (s, 6H), 2.03 (s, 12H).

Synthesis of 11,13-dimesityl-11,13-dihydro-3a2,11,13-triaza-6b,17b-diboraindeno[4',3',2',1':3,4,5]phenanthro[2,1,10,9-fghi]pentacene (**DoBN**)

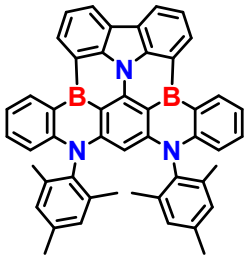

DoBN was synthesized according to the similar procedure of compound **3** by using compound 2 (401mg, 1 mmol) instead of compound 1. Final product **DoBN** was obtained as a yellow solid in 60% yield. ^{1}H NMR (500 MHz, $CDCl_3$) δ 9.21 (dd, *J* = 7.5, 1.5 Hz, 2H), 9.13 (d, *J* = 7.0 Hz, 2H), 8.51 (d, *J* = 7.5 Hz, 2H), 7.81 (t, *J* = 7.3 Hz, 2H), 7.53–7.46 (m, 2H), 7.36 (d, *J* = 7.3 Hz, 2H), 6.95 (s, 4H), 6.84 (d, *J* = 9.0 Hz, 2H), 5.36 (s, 1H), 2.44 (s, 6H), 1.73 (s, 12H). ^{13}C NMR (125 MHz, $CDCl_3$) δ 150.06, 145.95, 142.89, 141.72, 138.05, 136.63, 136.22, 135.54, 132.97, 131.71, 129.69, 125.28, 123.79, 123.13, 120.50, 115.79, 90.33, 21.29, 17.12.

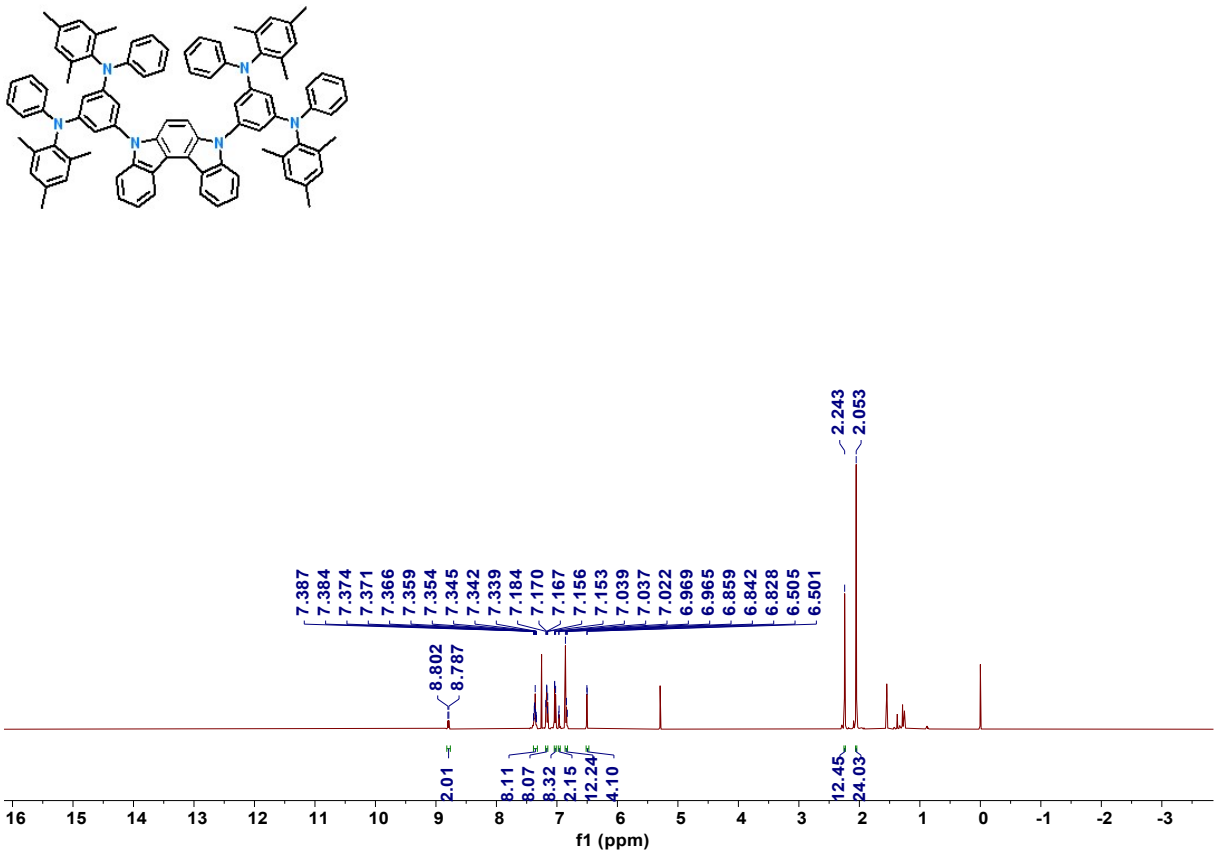

Figure S1. ^{1}H spectrum of compound **3** in $CDCl_3$.

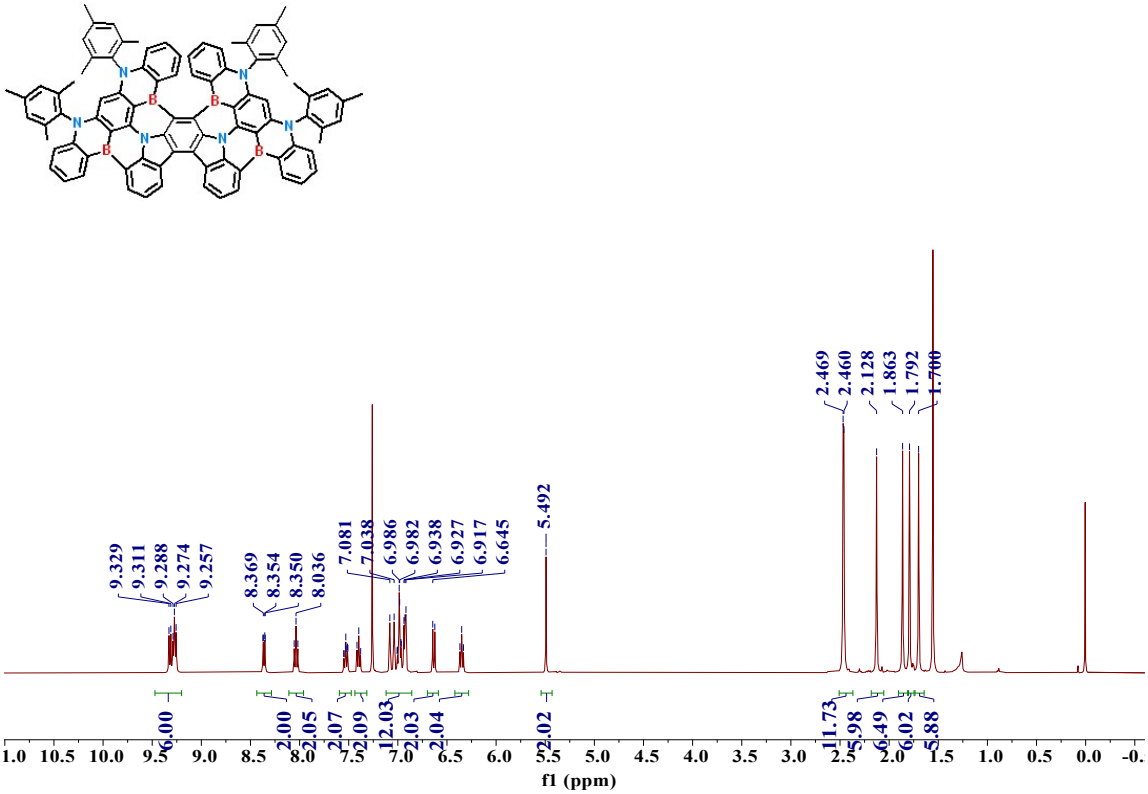

Figure S2. ^{1}H spectrum of **QuBN** in $CDCl_3$.

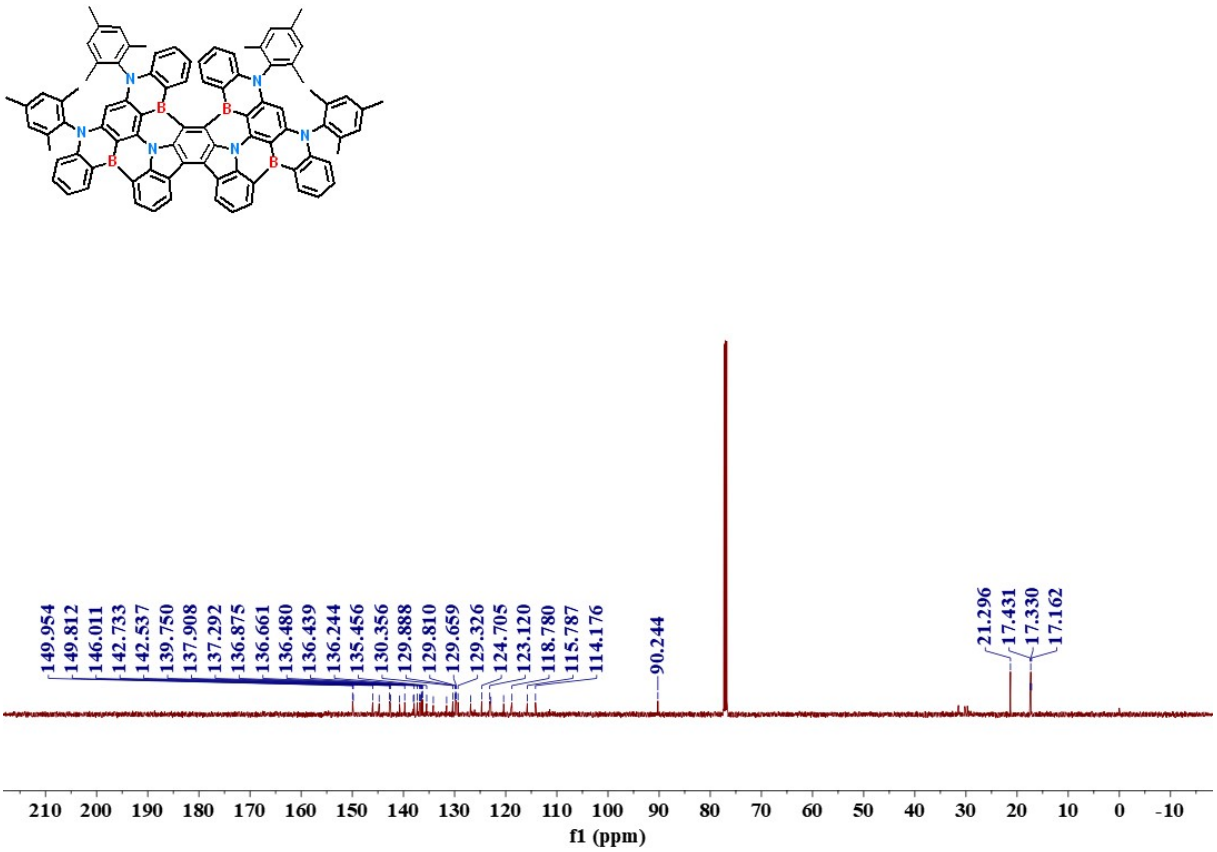

Figure S3. ^{13}C spectrum of **QuBN** in $CDCl_3$.

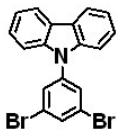

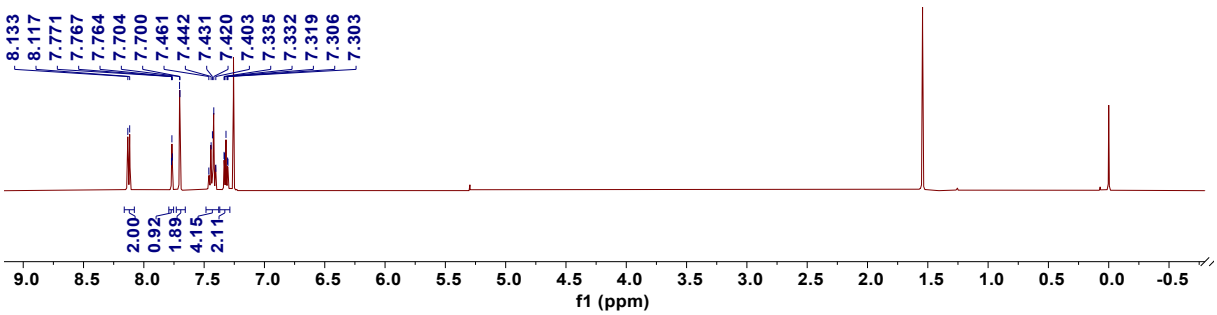

Figure S4. ^{1}H spectrum of compound **4** in $CDCl_3$.

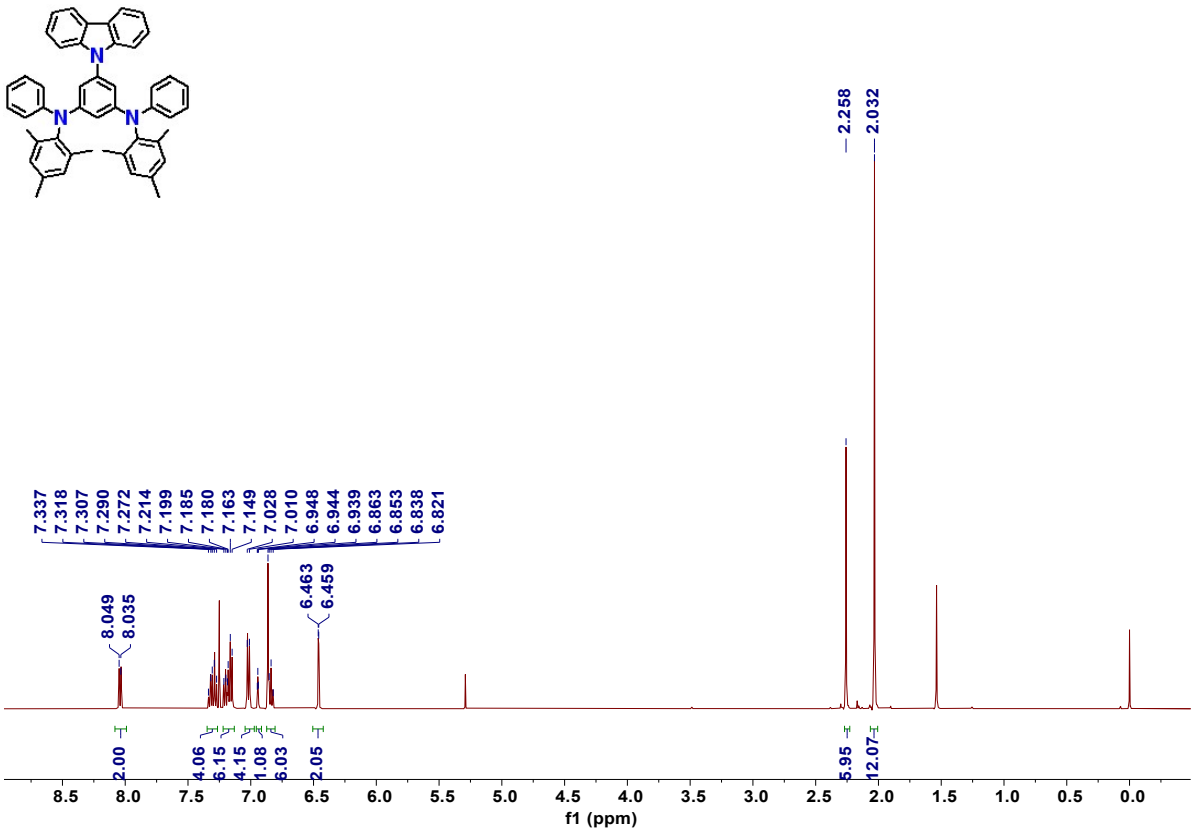

Figure S5. ^{1}H spectrum of compound **5** in $CDCl_3$.

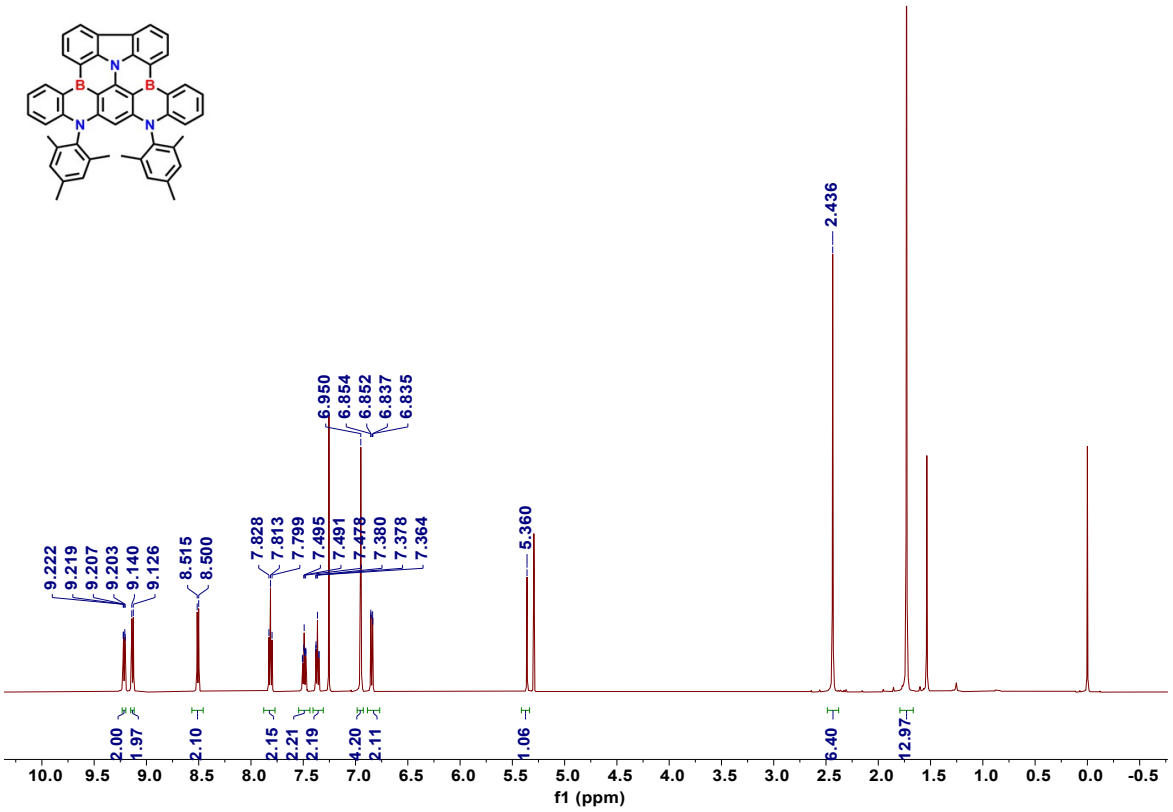

Figure S6. ^{1}H spectrum of **DOBN** in $CDCl_3$.

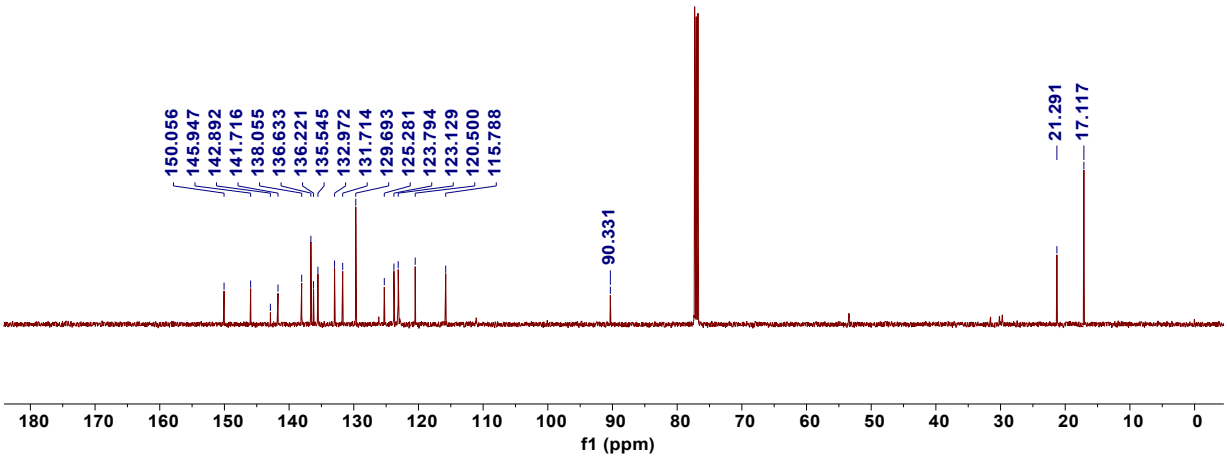

Figure S7. ^{13}C spectrum of **DOBN** in $CDCl_3$.

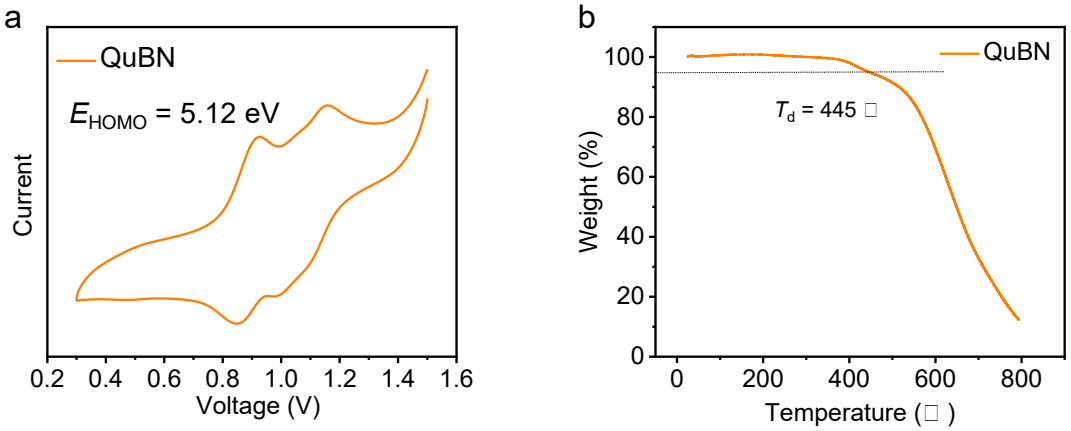

Figure S8. Cyclic voltammogram (CV) curve and thermogravimetric analysis (TGA) curve of **QuBN**.

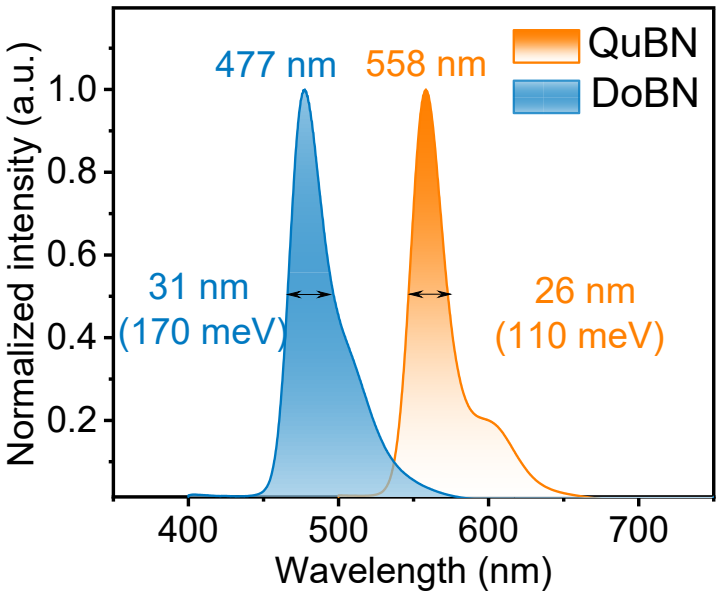

Figure S9. Photoluminescence spectra of **DoBN** and **QuBN** in 2 wt% doped DMIC-TRZ film.

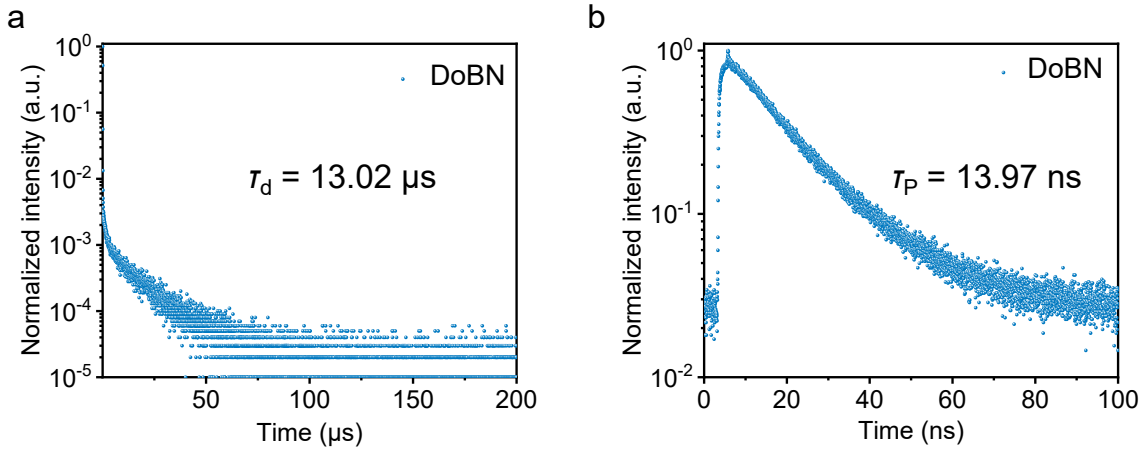

Figure S10. μs-Scale (a) and ns-scale (b) of transient photoluminescence curves for **DoBN** at room temperature in the film state (2 wt% doped in PMMA).

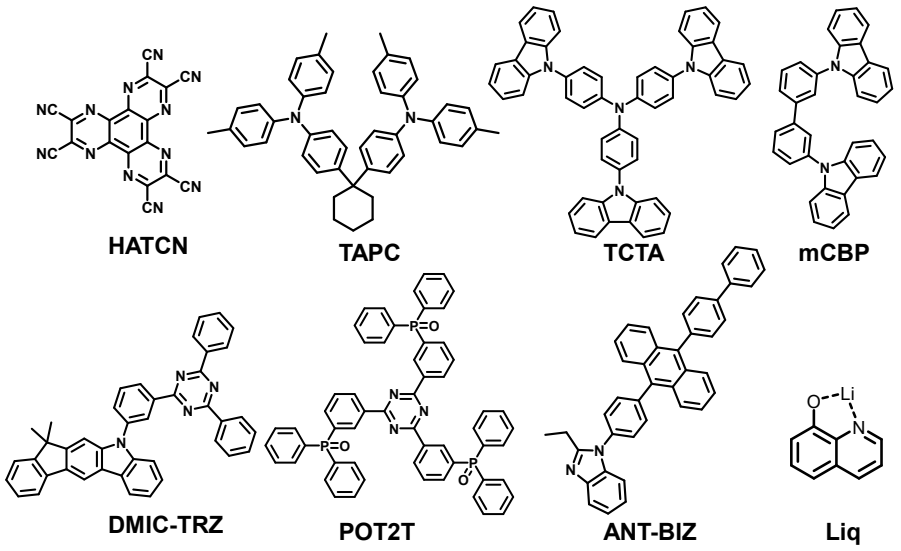

Figure S11. Chemical structures of functional layers.

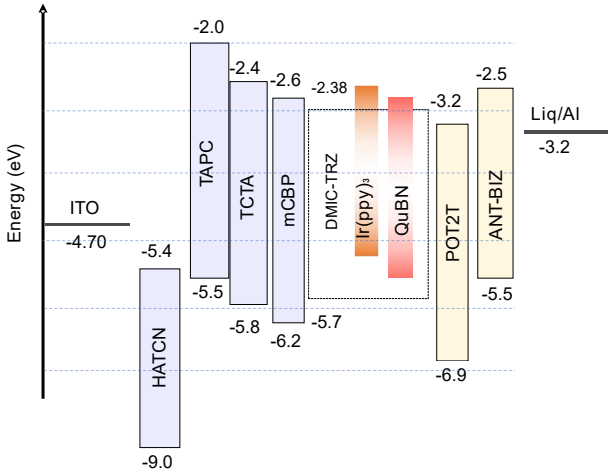

Figure S12. Detail architecture of HF device and the energies of each functional layers.

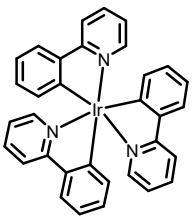

$Ir(ppy)_3$

Figure S13. Chemical structure of the sensitizer ($Ir(ppy)_3$).

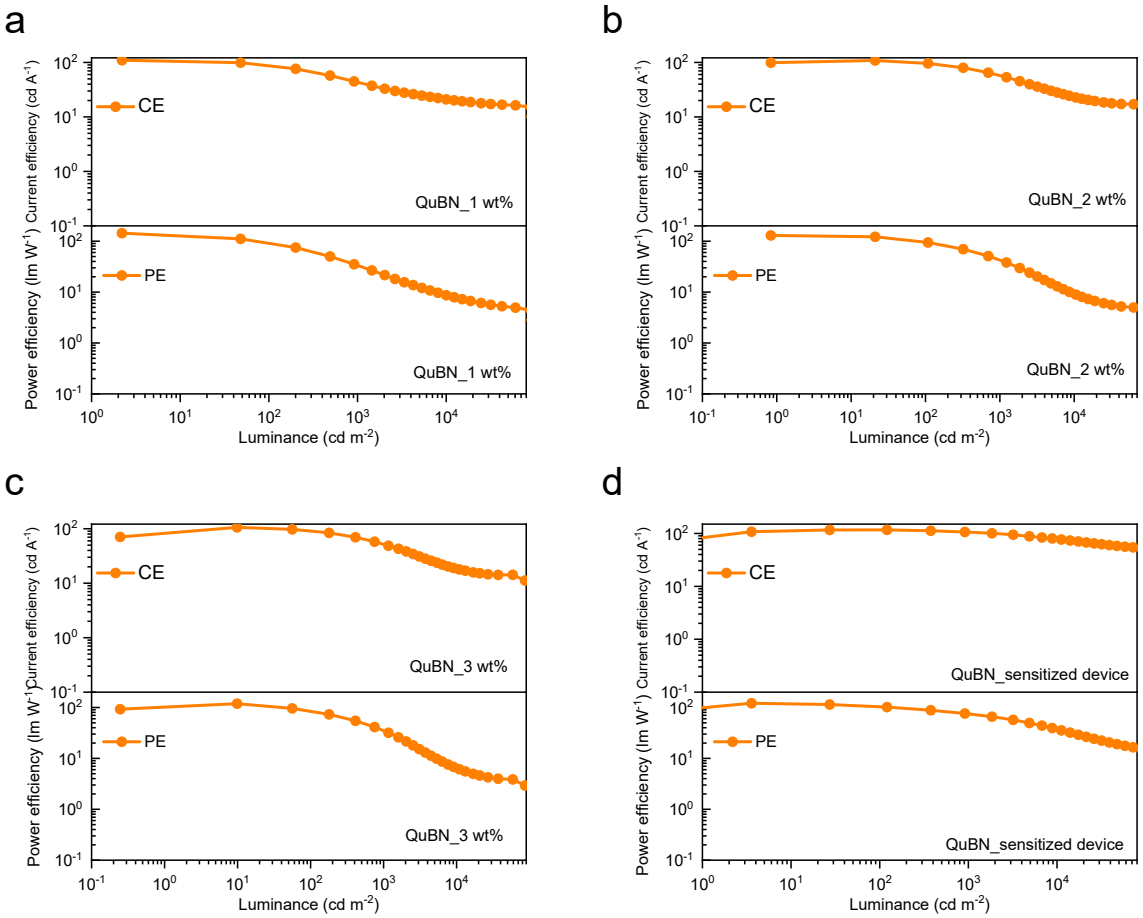

Figure S14. Current efficiency (CE) and power efficiency (PE) of **QuBN**-based devices. 1 wt% (a), 2 wt% (b), 3 wt% (c) and 2 wt%-doped HF devices (d).

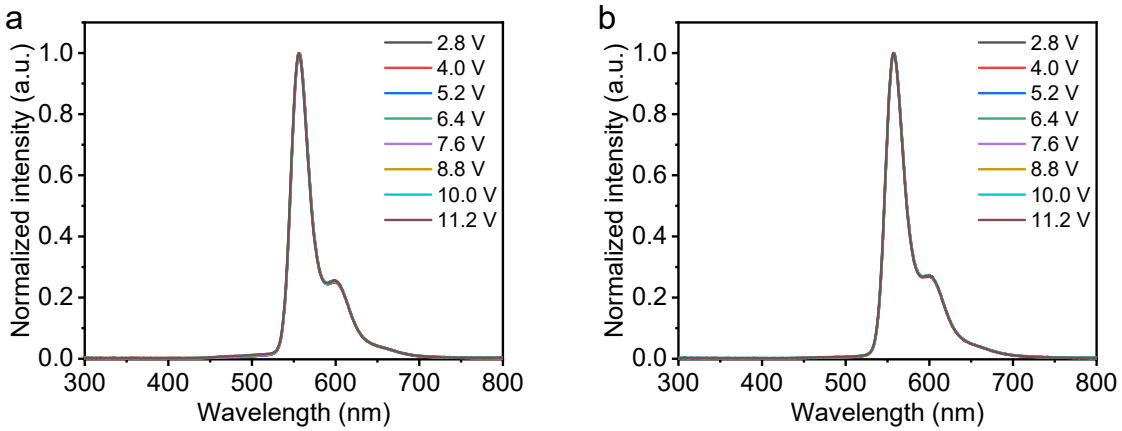

Figure S15. Normalized EL spectra at different operation voltages for **QuBN**-based non-sensitized (a) and HF (b) devices.

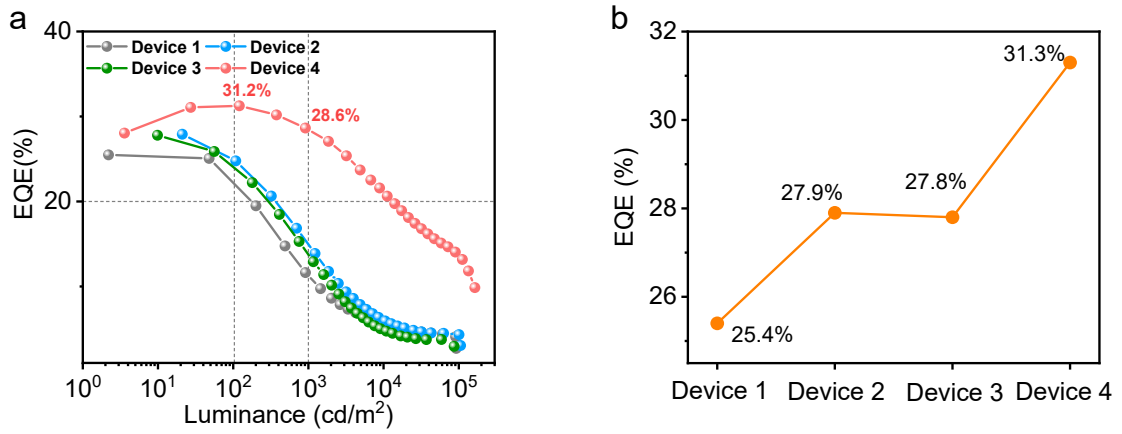

Figure S16. EL performance of **QuBN** at different conditions. Device 1: 1 wt% doped device; device 2: 2 wt% doped device; device 3: 3 wt% doped device; device 4: HF device.

Table S1 Crystal data and structure refinement for **QuBN** (CCDC number: 2545133).

Empirical formula	$C_{90}H_{68}B_4N_6$
Formula weight	1650.86
Temperature/K	170.00
Crystal system	orthorhombic
Space group	Pbca
a/Å	24.9430(13)
b/Å	32.1607(18)
c/Å	42.160(2)
α/°	90
β/°	90
γ/°	90
Volume/Å^3	33820(3)
Z	16
ρ_{calc}g/cm^3	1.297
μ/mm^{-1}	2.106
F(000)	13648.0
Crystal size/mm^3	0.13 × 0.08 × 0.06
Radiation	GaKα (λ = 1.34139)
2Θ range for data collection/°	6.72 to 108.218
Index ranges	$-30 \leq h \leq 26$, $-38 \leq k \leq 38$, $-39 \leq l \leq 50$
Reflections collected	265726
Independent reflections	30530 [R_{int} = 0.1432, R_{sigma} = 0.1122]
Data/restraints/parameters	30530/10/1825
Goodness-of-fit on F^2	1.364
Final R indexes [I>=2σ (I)]	R_1 = 0.1440, wR_2 = 0.3834
Final R indexes [all data]	R_1 = 0.2141, wR_2 = 0.4326
Largest diff. peak/hole / e Å^{-3}	0.96/-0.52

Table S2 Photophysical parameters of **QuBN**.

Emitter	λ_{abs}[a] [nm]	λ_{PL}[b] [nm]	FWHM[c] [nm]	E_{S1}[d] (eV)	E_{T1}[e] (eV)	ΔE_{ST}[f] (eV)	PLQY[g]	k_r[h] ($\times 10^7$ s^{-1})	k_{RISC}[i] ($\times 10^4$ s^{-1})
QuBN	540	552	20	2.34	2.14	0.20	91%	7.59	3.92

[a]Maximum absorption wavelength measured in toluene (10^{-5} M); [b]Maximum emission wavelength measured in toluene; [c]Full-width at half-maximum of the emission spectrum; [d]Singlet state energy estimated from 77 K; [e]Triplet state energy estimated from 77 K; [f]Singlet-triplet energy gap; [g]Photoluminescence quantum yield measured in 2 wt% doped film; [h]Rate constant of fluorescence radiative (k_r); [i]Rate constant of reverse intersystem crossing (k_{RISC})

Table S3 PLQYs of **QuBN** at different doping concentrations in the DMIC-TRZ host.

Doping concentration	1 wt%	2 wt%	3 wt%
PLQY	85%	91%	90%

References

1. Frisch, M. J. et al. Gaussian 16 Rev. C.01. (Gaussian, Inc., Wallingford CT, 2016).
2. M. Kállay, P. R. Nagy, D. Mester, Z. Rolik, G. Samu, J. Csontos, J. Csóka, P. B. Szabó, L. Gyevi-Nagy, B. Hégely, I. Ladjánszki, L. Szegedy, B. Ladóczki, K. Petrov, M. Farkas, P. D. Mezei, Á. Ganyecz, J. Chem. Phys. 2020, 152, 074107.
3. B. Li, J. Lou, B. Zhang, L. Liu, X. He, H. Xu, X. Feng, H. Zhang, Z. Wang, B. Z. Tang, *Chem. Eng. J.* 2024, *482*, 148876.